Digest Journal of Nanomaterials and Biostructures Vol. 11, No. 3, July – September 2016, p. 719 - 729

THEORETICAL PREDICTIONS OF THE STRUCTURAL, ENERGETIC AND ELECTRONIC PROPERTIES OF Ca-Sn, Sr-Sn AND Mg-Ca-Sr-Sn COMPOUNDS

X. M. DU[a*], R. Q. CHEN[a], L. L. LIU[b]
[a]*School of Materials Science and Engineering, Shenyang Ligong University, Shenyang 110159, China;*
[b]*Henan Mechnicial and Electrical Engineering College, Xinxiang 453003 , China.*

The structural, energetic and electronic properties of the binary intermetallic compounds in Ca-Sn, Sr-Sn systems and Mg_2Sn, Mg_2Sr, Mg_2Ca and ternary compounds MgCaSn and MgSrSn have been investigated by means of first-principles method within the framework of density functional theory. Based on the calculated results, the lattice constants, enthalpies of formation and cohesive energy for the these compounds were compared with previous experimental and theoretical investigations. It was indicated that Mg_2Sn phase has most stable structure and the strongest alloying ability of three Mg-alloys (Mg_2Sn, Mg_2Sr and Mg_2Ca). The structure stability of the binary Ca-Sn and Sr-Sn intermetallic compounds increases with decreasing Ca or Sr composition. Moreover, the stability of the ternary intermetallic compounds MgCaSn and MgSrSn which is the solid solution of Mg in Ca_2Sn and Sr_2Sn compounds, respectively, decreases in comparison with Ca_2Sn and Sr_2Sn. These results were also supported by the analysis of densities of states (DOS). DOS results indicated that the difference in stability for the Ca-Sn and Sr-Sn intermetallics could be attributed to the bonding electron numbers at the upper region of the valence band, which was cut by Fermi level. Moreover, the electronic structure of the Ca-Sn and Sr-Sn intermetallics also showed a strong hybridization between Ca-3d or Sr-3d and Sn-5p states, which played a significant role in the bonding mechanism of Ca-Sn, Sr-Sn, MgCaSn and MgSrSn intermetallics.

(Received May 29, 2016; Accepted July 8, 2016)

Keywords: First-principles; Intermetallics; Stability; Electronic structures

1. Introduction

The combination of light weight, high specific strength, and good castability makes magnesium alloys a promising engineering material for the automotive, weapon equipments, aerospace industries and other light-weight structural applications [1-3]. Strontium and calcium are two important additives used in magnesium alloys. The alloying effects of strontium on magnesium alloys, e.g. Mg–Al based alloys, have been found to display superior creep performance and excellent high-temperature properties [4]. Alloying magnesium with calcium, on the other hand, is suggested to improve the creep resistance and tensile strength, and to provide corrosion resistance comparable to commercial Mg-alloys with rare earth elements [5].

The Mg-Sn system is an age-hardenable alloy and exhibits good castability due to the eutectic nature of its phase diagram [6]. In recent years, significant improvements on the binary Mg-Sn and ternary Mg-Sn-Ca systems, in as-cast condition, have also been taken up for the purpose of achieving best combination of castability, creep and corrosion resistance [7−11].

*Corresponding author: du511@163.com

Investigations on the Mg_2Sn phase or on the Mg_2Sn, Mg_2Ca, Mg_2Sr and $Ca_{2-x}Mg_xSn$ phases that can be formed in binary Mg-Sn or in ternary Mg-Sn-Ca alloys have been performed as well. However, other precipitate phases such as $CaSn_3$, Ca_2Sn, CaSn in ternary Mg-Sn-Ca system and SrSn, Sr_2Sn, $SrSn_3$, Sr_5Sn_3 and MgSrSn in ternary Mg-Sn-Sr system which have an important influence on the stability, thermodynamic and mechanical properties of the ternary Mg-Sn-Ca, Mg-Sn-Sr alloys were rarely investigated theoretically and experimentally. Zhou et al. [12] carried out thermodynamic modeling of the Sn-Sr binary system and the Mg-Sn–Sr ternary system by means of the CALPHAD approach and obtained thermodynamic database and phase diagrams of the Sn-Sr binary system and the Mg-Sn–Sr ternary system. Zhao et al. [13] investigated the stability of six phases (Sr_2Sn, Sr_5Sn_3, SrSn, Sr_3Sn_5, $SrSn_3$ and $SrSn_4$) in Sn–Sr system by approach of CALPHAD and first-principles calculations. Yang et al. [14] experimentally found that the addition of minor Sr to the Mg-3Sn-2Ca (wt.%) alloy can suppress the formation of the primary CaMgSn phase and promotes the formation of Mg_2Ca phase.

For Sn-containing binary systems, such as Ca-Sn [15] and Sr-Sn [16] systems, there are many stable intermetallic compounds with much higher melting point than their constituent elements in these binary phase diagrams. It is possible that these intermetallic compounds in Ca-Sn, Sr-Sn systems have an important effect on microstructure and properties of Mg-based alloys. Unfortunately, these studies have not been reported up to present. In this work, the first-principles calculations are carried out to investigate the structural stabilities and electronic structures of 12 binary or ternary intermetallic compounds in Ca-Sn ($CaSn_3$, Ca_2Sn and CaSn) and Sr-Sn (Sr_2Sn, Sr_5Sn_3, SrSn and $SrSn_3$) systems, MgSnCa, MgSnSr, Mg_2Sn, Mg_2Sr and Mg_2Ca phases in order to better understand the alloying behavior of Ca or Sr on Mg-Sn alloys. The structures are optimized by full relaxation and the lattice parameters are obtained. The enthalpies of formation and cohesive energies are calculated and discussed. The density of states (DOS) is calculated to study the underlying mechanism of the structural stability. The study will give some theoretical guidance for the optimization and design of Mg-Sn alloys, and provide valuable estimation for the properties unavailable in experiments.

2. Computational methods

The calculations of the total energy and electronic structures were performed by the first-principles plane-wave pseudopotentials method based on density functional theory (DFT) [17] implemented in Quantum-ESPRESSO program package [18]. Ultrasoft pseudo-potential [19] was used to describe the ion-electron interaction. Generalized gradient approximation (GGA) [20] with the Perdew-Burke-Ernzerh (PBE) [21] was used to describe the exchange-correlation energy functional, and the precise testing calculations with a plane-wave cutoff energy of 380 eV have been performed. Brillouin Zone integrations were performed using the Monkhorst-Pack [22] k-point meshes, e.g., the k-point meshes for Mg_2Sn, Mg_2Sr, Mg_2Ca, $CaSn_3$, Ca_2Sn, CaSn, Sr_2Sn, Sr_5Sn_3, SrSn, $SrSn_3$, MgCaSn and MgSrSn were 6×6×6, 8×8×6, 8×8×6, 8×8×8, 6×8×4, 10×10×10, 6×9×5, 6×6×5, 11×11×11, 6×6×6, 8×8×7 and 8×8×7, respevtively. All lattice parameters and atomic positions in our models have been relaxed according to the total energy and force using the Broyden-Flecher-Goldfarb-Shanno (BFGS) [23] scheme. The convergence criteria for geometry optimization was as follows: electronic self-consistent field (SCF) tolerance less than 5.0×10^{-5} eV/atom, Hellmann-Feynman force below 0.01eV/Å, maximum stress less than 0.05GPa and displacement within 2.0×10^{-4} Å. After the structures were optimized, the total energies were recalculated self-consistently with the tetrahedron method. The latter technique was also used to calculate the electronic density of states (DOS).

3. Results and discussion

3.1 Crystal structures

In the present work, the original crystal structures have been built based upon the experimental crystallographic data of twelve stable phases: Mg_2Sn, Mg_2Sr, Mg_2Ca, $CaSn_3$, Ca_2Sn, CaSn, Sr_2Sn, Sr_5Sn_3, SrSn, $SrSn_3$, MgCaSn and MgSrSn [24-34]. Starting from the above crystal structure, the structural optimization was first performed by full relaxation of cell shape and atomic positions. The optimized lattice parameters are listed in Table 1, where the available experimental and other theorectic results are also presented. It can be found that the present calculated lattice constants are in good agreement with the available experimental and theoretical values [12,13, 24-36], with a difference within 2.0%, confirming that the computational methodology utilized in this work is highly suitable and reliable.

Table 1 Optimized, experimental and other calculated lattice parameters

Alloys	Space group	Lattice parameters(Å)								
		Present			Exp.			Cal.		
		a	b	c	a	b	c	a	b	c
Mg_2Sn	*Fm-3m*	6.858			6.759[24]			6.825[35]		
Mg_2Sr	*P6$_3$/mmc*	6.457		10.422	6.475		10.430[25]	6.468		10.466[36]
Mg_2Ca	*P6$_3$/mmc*	6.278		10.185	6.271		10.170[26]	6.234		10.034[35]
$CaSn_3$	*Pm-3m*	4.766			4.732[27]					
Ca_2Sn	*Pnma*	7.965	5.062	9.605	7.975	5.044	9.526[28]			
CaSn	*Cmcm*	4.821	11.648	4.356	4.821	11.520	4.349[29]			
$SrSn_3$	*R-3m*	6.975		33.45	6.940		33.01[30]	7.002		33.394[12]
Sr_2Sn	*Pmnm*	8.382	5.432	10.271	8.402	5.378	10.078[31]	8.428	5.408	10.148[13]
								8.426	5.407	10.167[12]
SrSn	*Cmcm*	5.112	12.338	4.507	5.045	12.04	4.494[32]	5.112	12.187	4.525[13]
								5.089	12.200	4.545[12]
Sr_5Sn_3	*I4/mcm*	8.586		16.391	8.565		16.261[33]	8.608		16.528[13]
								8.613		16.531[12]
MgSnCa	*Pnma*	7.878	4.735	8.818	7.860	4.660	8.740[34]			
MgSnSr	*Pnma*	8.355	4.932	8.980	8.180	4.920	8.750[34]	8.221	4.896	8.918[12]

3.2 Enthalpies of formation and cohesive energies

To estimate structural stability of twelve compounds, the cohesive energy was calculated. The cohesive energy is defined as the energy that is needed when the crystal is decomposed into a single atom. The lower the cohesive energy is, the more stable the crystal structure is. The cohesive energy was calculated as

$$E_{coh} = (E_{tot} - N_A E_{atom}^A - N_B E_{atom}^B) / (N_A + N_B) \quad (1)$$

where E_{tot} is the total energy of the unit cell, E_{atom}^A and E_{atom}^B are the total energies of the isolated atoms A and B in free state. N_A and N_B refer to the number of A and B atoms in unit cell, respectively. Thelower the cohesive energy corresponds to the stronger structural stability.

The enthalpy of formation (ΔH) per atom of these compounds was also calculated to estimate the alloying ability of crystal

$$\Delta H = (E_{tot} - N_A E^A_{solid} - N_B E^B_{solid}) / (N_A + N_B) \quad (2)$$

where E^A_{solid} and E^B_{solid} are the energy per atom of pure solid states *A* and *B*, respectively. other quantities are the same as defined in Eq. (1). Negative enthalpies of formation usually means an exothermic process, and lower enthalpies of formation corresponds to stronger alloying ability.

The calculated enthalpies of formation and cohesive energies of these compounds are listed in Table 2, together with the available experimental and other calculated values [12, 13, 37, 38, 40-45]. It should be noted that the experimental values of the enthalpies of formation and cohesive energies for Sr-Sn compounds were not reported. As can be seen from Table 2, the calculated values in this work are in good agreement with the experimental and theoretical values for Mg_2Sn, Mg_2Sr and Mg_2Ca phases. Moreover, the calculated enthalpies of formation are also in good agreement with the reported values in Ref. [12, 13, 44, 45] for Sr-Sn and Ca-Sn compounds. For Mg_2Sn, Mg_2Sr and Mg_2Ca compounds, it can be found that Mg_2Sn has most stable structure and the strongest alloying ability, then Mg_2Ca, finally Mg_2Sr. Fig. 1 presents the calculated enthalpies of formation and cohesive energies for the Ca-Sn compounds. It is found that the absolute values of cohesive energies increase with the increase of Sn content in various Ca-Sn compounds, indicating the structural stability of these compounds increases. $CaSn_3$ has most stable structure. However, change of enthalpy of formation is not monotonous as the content of Sn increases. CaSn has the strongest alloying ability in Ca-Sn compounds. In Sr-Sn compounds, the cohesive energies and enthalpies of formation show the same change trend as Ca-Sn compounds, as also shown in Fig.2. $SrSn_3$ has most stable structure. SrSn has the strongest alloying ability in Sn-Sn compounds. It should be noted here that the enthalpy of formation for Sr_5Sn_3 is slightly above the convex hull between Sr_2Sn and SrSn compounds. The phenomenon was also observed by Zhao et al. [13] at room temperature for Sr-Sn system. It is explained that Sr_5Sn_3 should be metastable at room temperature, and there exists a solid-state transformation, Sr_5Sn_3 = Sr_2Sn + SrSn.

In the Mg-Ca-Sn system, the " ternary compound " MgCaSn is actually found to be the solid solution of Mg in Ca_2Sn [46]. The crystal structure of MgCaSn compound was reported as Pnma space group [46]. In the Mg-Ca-Sn thermodynamic modeling work by Kozlovetal. [46], the MgCaSn and Ca_2Sn phases were modeled as a ternary solid solution $Mg_xCa_{2-x}Sn$ using a sublattice model (Ca)(Ca, Mg)(Sn) which terminates at the composition x=1, i.e. MgSnCa. For Mg-Sn-Sr system, there are no experimental data for the Mg-Sr-Sn ternary system except the existence of the MgSrSn compound. Eisenmann et al. [34] synthesized the MgSrSn compound and determined its crystal structure to be orthorhombic anti-$PbCl_2$ type, which is similar to the crystal structure of MgCaSn compound reported in the Mg-Ca-Sn system [46]. Meanwhile, in the Mg-Sr-Sn system, which is similar to the Mg-Ca-Sn system, the crystal structures of MgSrSn and $SnSr_2$ share the same Pnma space group. Zhou et al.[12] treated MgSrSn and $SnSr_2$ as a ternary solid solution $Mg_xSr_{2-x}Sn$ in thermodynamic modeling using a sublattice model (Sr)(Sr,Mg)(Sn). In present work, we also treat the ternary compounds MgCaSn and MgSrSn as ternary solid solution $Mg_xCa_{2-x}Sn$ and $Mg_xSr_{2-x}Sn$ which terminate at the composition x=1. The calculated the enthalpies of formation and cohesive energies for MgCaSn and MgSrSn are larger than that of Ca_2Sn and Sr_2Sn,

respectively, as also shown in Table 2. This indicates that the solid solution of Mg in Ca_2Sn and Sr_2Sn compounds decreases their stabilites. Moreover, the calculated formation enthalpies of MgCaSn and MgSrSn are in fairly good agreement with the assessed value of Ref. [12,46], which strongly supports the reliability of the present first-principle calculations. It is to be noted that the tabulated data in Ref. [46] for the enthalpy of formation correspond to the value at 298 K, while the first-principle data for MgCaSn phase shown in Table 2 are the formation enthalpy at 0 K. The inclusion of vibrational contributions lead to slightly more negative enthalpy of formation at 298 K as expected.

Table 2 Calculated total energies E_{tot} and enthalpies of formation ΔH and cohesive energies E_{coh} for twelve compounds

Phases	E_{tot} (eV)	E_{coh} (kJ/mol)		ΔH (kJ/mol)		
		Present	Cal.	This work	Expt.	Cal.
Mg_2Sn	-2043.9914	-234.82	-251.83[37]	-18.04	-24.3[40]	-20.82[40]
Mg_2Sr	-11138.3507	-149.63	-156.80[38]	-11.80	-7.95[41]	-10.62[42]
Mg_2Ca	-11799.3654	-157.98	-167.83[43]	-11.95	-	-11.34[43]
$CaSn_3$	-1289.7655	-338.87		-41.65	-44.98±4.2[44]a	-40.94 [45] a
Ca_2Sn	-8402.2076	-288.65		-63.48	-104.6±12.6[44]a	-66.36 [45] a
CaSn	-2196.7239	-317.24		-63.82	-79.5±10.5[44]a	-66.32 [45] a
$SrSn_3$	-4498.1263	-327.83		-42.02	-	-41.641[12]
						-41.74[13]
Sr_2Sn	-7080.2629	-253.99		-63.86	-	-63.40[13]
						-61.76[12]
SrSn	-1866.3605	-294.08		-67.07	-	-68.88[13]
						-67.61[12]
Sr_5Sn_3	-8946.4714	-263.13		-63.74	-	-64.47[13]
						-63.02[12]
MgSnCa	-8290.7860	-267.29		-54.43	-	-56.89[46]a
MgSnSr	-7630.1168	-252.27		-57.05	-	-56.56[12]

[a] 298K, 0 GPa.

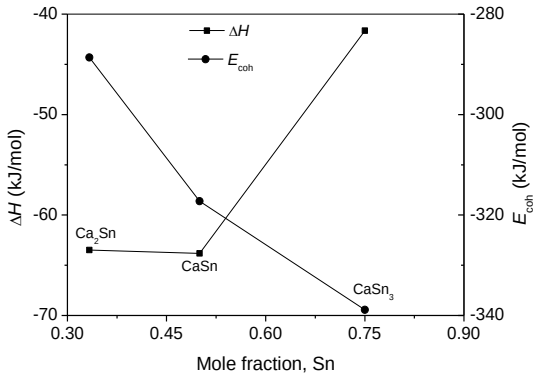

Fig. 1 The calculated enthalpies of formation and cohesive energies for various Ca–Sn compounds

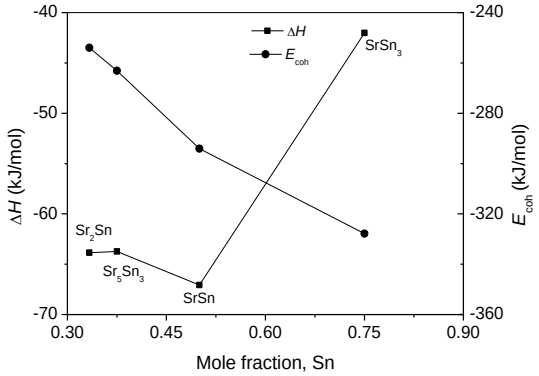

Fig. 2 The calculated enthalpies of formation and cohesive energies for various Sr–Sn compounds

3.3 Electronic structures

Usually, structural stability of intermetallic compounds depends on the bonding electron orbital characteristics. For covalent bond, it depends on the depth and width of band gap near Fermi level, while ionic bonds are decided by transfer charge for different atoms. In the present work, the electronic structures were calculated to gain a further insight into the bonding of Sn-Ca, Sn-Sr compounds, MgCaSn, MgSrSn, Mg_2Sn, Mg_2Sr and Mg_2Ca, and then to reveal the underlying structural stability mechanism of these compounds. The total and partial densities of states (DOS and PDOS) of these compounds are presented in Fig. 3 to Fig. 6. From Fig.3, it is found that the main bonding peaks of Mg_2Sr, Mg_2Sn and Mg_2Ca locate in the range from −10 eV to 0 eV, originating from the contribution of valance electron numbers of Mg-2s, Mg-2p, Sr-3d orbits; Mg-2s, Mg-2p, Sn-5s and Sn-5p orbits; Mg-2s, Mg-2p, Ca-3d, respectively. The values of the total DOS at Fermi level are larger than zero for Mg_2Sr, Mg_2Sn and Mg_2Ca phases, which indicats the metallic behavior. The bonding electron numbers at the Fermi level, $N(E_F)$ for Mg_2Sr, Mg_2Sn and Mg_2Ca phases is 9.33, 0.64 and 8.51, respectively. In general, $N(E_F)$ on DOS plot can be used to characterize the activity of valance electrons of the atoms in crystal. Namely, the smaller $N(E_F)$, the less is change probability of the electronic structures of the crystal when external conditions change, thus the crystal has the higher stability [47]. The stability of Mg_2Sn phase is stronger than that of Mg_2Sr or Mg_2Ca, which are entirely consistent with the results of the calculated enthalpies of formation cohesive energies.

Fig. 4 and Fig.5 show the calculated DOS of Ca-Sn and Sr-Sn systems. It is found that the total DOS at the Fermi level is not zero and no band gap occurs in the vicinity of Fermi level. Consequently, the these compounds are all metallic. More importantly, the shape of the valence bands located between -5 eV and 0 eV can be formed due to a strong bonding between Ca-3d (or Sr-3d) states and Sn-5p states, which may form typical hybridized p-d states, and a deep valley or pseudogap separates the bonding and antibonding states. Obviously, the p-d hybridization of Ca-Sn and Sr-Sn intermetallic compounds is an important atomic characteristic of strong covalent bonding between Ca (or Sr) and Sn and hence the electronic origin for high stability of Ca-Sn and Sr-Sn compounds. For MgCaSn and MgSrSn compounds, the total and partial densities of states of the two phases are similar to Ca_2Sn and Sr_2Sn, respectively, as shown in Fig. 6. The valence bands located between -5 eV and 0 eV mainly are dominated by Mg-2s, Mg-2p, Sn-5p and Ca-3d (or Sr-3d) orbit electrons. The valence bands of MgCaSn and MgSrSn compounds become wider than that of Ca_2Sn and Sr_2Sn.

From Fig. 4 to Fig. 6, it can be also that the total DOS plots are divided into three energy regions: (i) Region 1, the lowest region stemming mainly from Sn 5s states; (ii) Region 2, the upper region of the valence band is cut by Fermi level and is mainly due to valence electron numbers of Ca-3d (or Sr-3d) mixed with Sn 5p states; and (iii) Region 3, the energy region just above Fermi level dominated by unoccupied 3d alkaline-earth metals states. It can be easily found that Region 2 gradually becomes narrow in the total DOS for the Ca-Sn and Sr-Sn compounds

with adding Ca or Sr, while Region 1 is the opposite. It is further revealed that the number of bonding electrons in Regions 2 decreases with an increase of Ca-3d or Sr-3d electrons, indicating that the stability of the crystals increases, which well corresponds to the variation in cohesive energies of the compounds mentioned above. Moreover, by analyzing the bonding electron number of per atom in Region 2 for Ca-Sn i.e., 2.154 for Ca_2Sn, 2.021 for CaSn, 1.990 for $CaSn_3$, respectively and Sr-Sn compounds, i.e., 2.152 for Sr_2Sn, 2.064 for Sr_5Sn_3, 2.023 for SrSn and 1.952 for $SrSn_3$, respectively. It can be found that the value gradually decreases with the decreasing of Ca or Sr content, which is also consistent with the variation in cohesive energies of the compounds. The bonding electron numbers of per atom in Region 2 for MgCaSn and MgSrSn is 2.204 and 2.202, respectively, which is larger than that of Ca_2Sn and Sr_2Sn, respectively. This also indicates that the stability of MgCaSn and MgSrSn decreases in comparison with Ca_2Sn and Sr_2Sn. Thus, we can draw a conclusion that different levels of stability between these compounds could be attributed to the bonding electron numbers (the majority being Ca or Sr 3d electrons) at the upper region of the valence band that is cut by the Fermi level (Region 2).

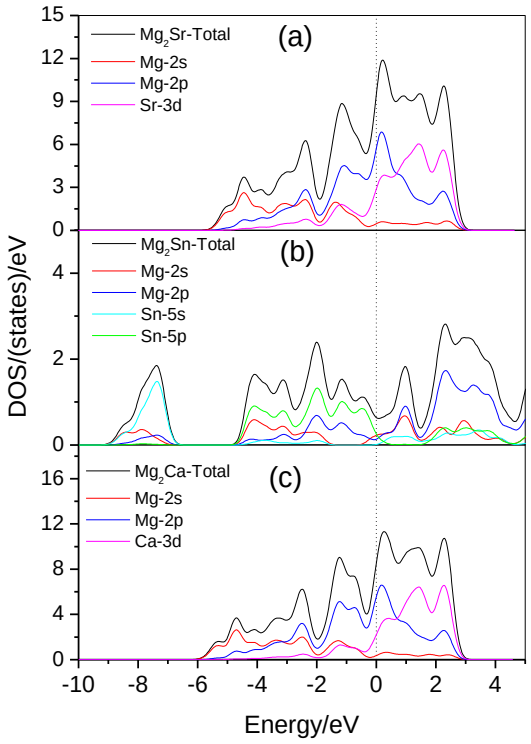

Fig.3 Calculated density of state (DOS) of: (a) Mg_2Sr, (b) Mg_2Sn, (c) Mg_2Ca

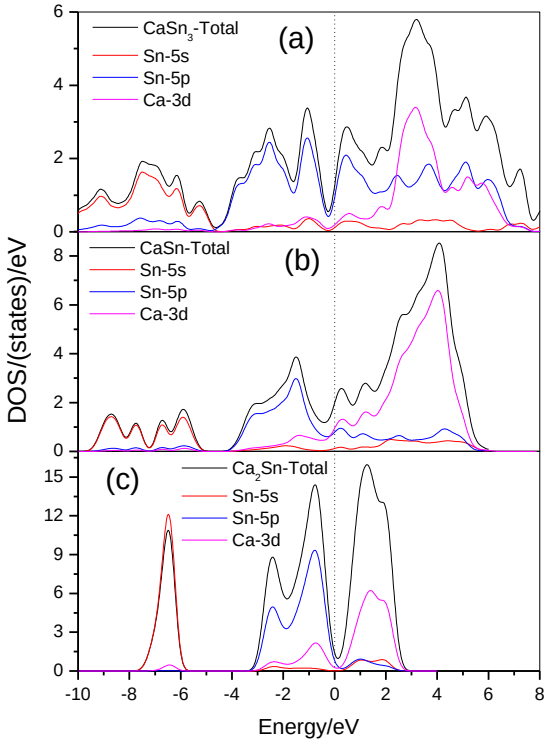

Fig.4 Calculated density of state (DOS) of: (a) $CaSn_3$, (b) CaSn, (c) Ca_2Sn

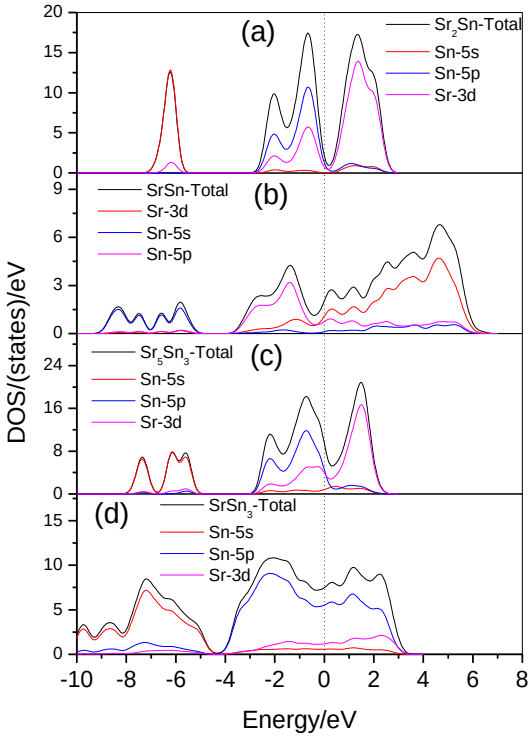

Fig.5 Calculated density of state (DOS) of: (a) Sr_2Sn; (b) SrSn, (c) Sr_5Sn_3, (d) $SrSn_3$

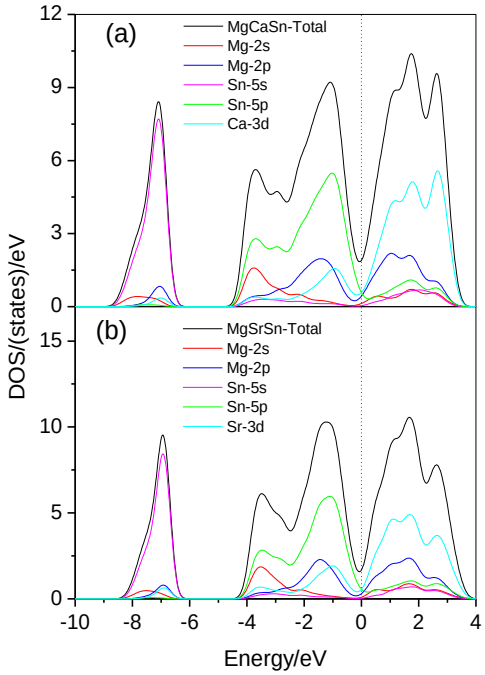

Fig.6 Calculated density of state (DOS) of: (a) MgCaSn, (b) MgSrSn

4. Conclusions

First-principle calculations of structural, energetic and electronic properties for 12 binary or ternary intermetallic compounds in Sn-Ca ($CaSn_3$, Ca_2Sn and CaSn) and Sn-Sr (Sr_2Sn, Sr_5Sn_3, SrSn and $SrSn_3$) systems, MgCaSn, MgSrSn, Mg_2Sn, Mg_2Sr and Mg_2Ca have been conducted. The calculated equilibrium lattice constants for these compounds are in good agreement with the available experimental and theoretical values. The results of cohesive energy show Mg_2Sn has most stable structure and the strongest alloying ability for Mg_2Sn, Mg_2Sr and Mg_2Ca. The structure stability of the binary Ca-Sn and Sr-Sn intermetallic compounds increases with decreasing Ca or Sr composition. Moreover, the stability of the ternary intermetallic compounds MgCaSn and MgSrSn which is the solid solution of Mg in Ca_2Sn and Sr_2Sn compounds, respectively, decreases in comparison with Ca_2Sn and Sr_2Sn. These conclusions has also been confirmed according to electronic properties obtained by the analysis of DOS and bonding electrons. The difference of stability between intermetallic compounds could be traced back to the bonding electron numbers at the upper region of the valence band that is cut by the Fermi level. It is also revealed from the electronic structure that a strong bonding between Ca-3d or Sr-3d states and Sn-5p states, which forms a typical hybridized p-d state.

Acknowledgement

The authors gratefully acknowledge the Project supported by the Natural Science Foundation of Liaoning Province, China.

References

[1] B.L. Mordike, T. Ebert, Mater. Sci. Eng. **A302**, 37 (2001).

[2] K. Kainer, H. Dieringa, J. Bohlen, N. Hort, D. Letzig, Magnesium Technology 2007, ed. R. S. Beals, A. A. Luo, M. O. Pekguleryuz, N. R. Neelameggham, 3-8, Warrendale, PA: TMS, 2007.

[3] K.U. Kainer, editor, Magnesium: Proc. 7th Internat. Conference on Magnesium Alloys and their Applications,Weinheim, Germany: Wiley-VCH Verlag, 2007.

[4] E. Baril, P. Labelle, M. O. Pekguleryuz, J. Miner. Metals Mater. Soc., JOM, **55**, 34 (2003).

[5] M. O. Pekguleryuz, J. Renaud, Creep Resistance in Mg–Al–Ca casting alloys, in: Magnesium 2000 Symposium, J. Miner. Metals Mater. Soc., TMS **2000**, 279 (2000).

[6] M. Bamberger, G. Dehm, Ann. Rev. Mater. Res., **38**, 505 (2008).

[7] A. L. Bowles, H. Dieringa, C. Blawert, N. Hort, K. U. Kainer, Mat. Sci. Forum **488/489**, 135 (2004).

[8] A. Kozlov, M. Ohno, T. A. Leil, N. Hort, K. U. Kainer, R. Schmid-Fetzer, Intermetallics **16**, 316 (2008).

[9] N. Hort, Y. Huang, T. A. Leil, P. Maier, K U. Kainer, Adv Eng Mat, **8**, 359 (2006).

[10] C. L. Mendis, C. J. Bettles, M. A. Gibson, C. R.Hutchinson, Mat Sci Eng A **435/436**, 163 (2006).

[11] H. Liu, Y. Chen, Y. Tang, D. Huang, G. Niu, Mat Sci Eng A **437**, 348 (2006).

[12] B. C. Zhou, S. L. Shang, Z. K. Liu, CALPHAD: Computer Coupling of Phase Diagrams and Thermochemistry **46**, 237 (2014).

[13] J. Zhao, Y. Du, L. Zhang, A. Wang, L. Zhou, D. Zhao, J. Liang, Thermochimica Acta **529**, 74 (2012).

[14] M. Yang, H. Li, C. Duan, China Foundry **11**, 108 (2014).

[15] H. Okamoto, Journal of Phase Equilibria **22**, 589 (2001).

[16] H.Okamoto, J. Phase Equilib. Diffus. **27**, 205 (2006).

[17] W. Kohn, L. J. Sham, Phys. Rev. A. **140**, 1133 (1965).

[18] http://www.pwscf.org.

[19] S. B. Fagan, R. Mota, R. J. Baierle, J. Molecular Struct. **539**, 101 (2001).

[20] J. D. Pack, H. J. Monkhors, Phys. Rev. B **16**, 748 (1977).

[21] J. P. Perdew, K. Burke, M. Ernzerh, Phys. Rev. Lett. **77**, 3865 (1996).

[22] H. J. Monkhorst, J. D. Pack, Phys. Rev. B **13**, 5188 (1976).

[23] T. H. Fischer, J. Alml, J. Phys. Chem. **96**, 9768 (1992)

[24] G. H. Grosch, K. J. Range, J. Alloys Compd. **235**, 250 (1996).

[25] M. M. Makhmudov, O. I. Bodak, A.V. Vakhobov, T. D. Dzhurayev, Russ. Metall. **6**, 209 (1981).

[26] F. Gingl, K. Z.Yvon, Kristallogr. **206**, 313 (1993).

[27] E. Zintl, S. Z. Neumayr, Elektrochem. Angew. Phys. Chem. **39**, 86 (1933).

[28] P. Eckerlin, E. Leicht, E. R. Wölfel, Z. Anorg. Allg. Chem. **307**, 145 (1961).

[29] P. Eckerlin, H. J. Meyer, E. R. Wölfel, Z. Anorg. Allg. Chem. 281, 322 (1955).

[30] T. F. Fässler, S.Hoffmann, Z. Anorg. Allg. Chem. **626**, 106 (2000).

[31] A.Widera, H. Schäfer, J. Less-Common Met. **77**, 29 (1981).

[32] P. Villars, PaulingFile, <http://crystdb.nims.go.jp>, 2004.

[33] G.Bruzzone, E. A. Franceschi, F. Merlo, J. Less-Common Met. **60**, 59 (1978).
[34] B. Eisenmann, H. Schäfer, A. Weiss, Z. Anorg. Allg. Chem. **391**, 241 (1972).
[35] H. Zhang, J. Saal, A. Saengdeejing, Y. Wang, L.Q. Chen, Z. K. Liu, ed. R. S. Beals, A. A. Luo, M. O. Pekguleryuz, N. R. Neelameggham, 345-350, Warrendale, PA: TMS, 2007.
[36] P. Mao, B.Yu, Z. Liu, W. Feng, J. Yang, J. Appl. Phys. **117**, 115903 (2015).
[37] D. Zhou, S. Xu, F. Zhang, P. Peng, J. Liu, Acta Metallurgica Sinica **46**, 97 (2010).
[38] D. Zhou, J. Liu, S. Xu, P. Peng, Acta Metallurgica Sinica **47**, 1315 (2011).
[39] W. Yu. Electronic structure and mechanical properties of Mg−Al−Ca Laves phase and Mg−Al−Sb alloys [D]. Xiangtan: Xiangtan University, 2009. (in Chinese)
[40] H. Zhang, S. Shang, E. S. James, A. Saengdeejing, Y. Wang, L. Chen, Z. Liu, Intermetallics **17**, 878 (2009).
[41] M. Aljarrah, M. Medraj, Comp Coup Phase Diagrams Thermochem **32**, 240 (2008).
[42] Y. Zhong, J. O. Sofo, A. A. Luo, Z. K. Liu. J. Alloys Compd. **421**, 172 (2006).
[43] P. Mao , B. Yu, Z. Liu, W. Feng, J.Yang, J. Magneuium and Alloys. **1**, 256 (2013).
[44] O. Kubaschewski, Villa H. Z Elektrochem **53**, 32 (1949).
[45] M. Ohno, A. Kozlov, R. Arroyave, Z. K. Liu, R. Schmid-Fetzer, Acta Materialia **54**, 4939 (2006).
[46] A. Kozlov, M. Ohno, R. Arroyave, Z. K. Liub, R. Schmid-Fetzer, Intermetallics **16**, 299 (2008).
[47] Y. Imai, M. Mukaida, T. Tsunoda, Intermetallics, **8**, 381 (2000).